Maser Observations to Probe Massive Star Formation in G354.61+0.47

M. Hafieduddin[1,2]*, T. Hirota[3,4], T. Hidayat[1,2] and K. Sugiyama[3,5]

[1]*Astronomy Research Group, FMIPA ITB, Bandung, Indonesia*
[2]*Bosscha Observatory, FMIPA ITB, Lembang, Indonesia*
[3]*Mizusawa VLBI Observatory, NAOJ, Tokyo, Japan*
[4]*The Graduate University for Advanced Studies, SOKENDAI, Hayama, Japan*
[5]*National Astronomical Research Institute Thailand, NARIT,Chiang Mai, Thailand*
**E-mail*: mhafieduddin@gmail.com

ABSTRACT

Massive stars, or stars with mass more than $8M_{\odot}$, have great impact both in local and cosmological scale. But the modelling of their formation is hindered by the rarity of data. The advance of *Very Long Baseline Interferometry* (VLBI) helps us overcome this problem by enabling us to observe structure tracer with high angular resolution. In this research, we use data taken with *KVN and VERA Array* (KaVA), *East-Asian VLBI Network* (EAVN), and *Atacama Large Millimeter/submillimeter Array* (ALMA) to probe structures in massive star formation region G354.61+0.47. We combine the 22 GHz H_2O maser data taken with KaVA with the 6.7 GHz CH_3OH maser data taken with EAVN and then compare them with continuum and CO (*J=3*-2) emission line data taken with ALMA. Calibrations, data processing, and imaging are conducted using AIPS and CASA software. Proper motions are then measured accordingly. We found that H_2O maser distribution is approximately perpendicular in the east side of elliptical distribution of CH_3OH maser and its position and proper motion agree with outflow structure traced by CO (*J*=3-2) line. Comparison with ALMA continuum map leads us to conclude so far that CH_3OH maser distribution traces circumstellar disk structure and H_2O maser distribution shows us a more general motion of the gases, such as outflows, expansion or turbulence.

Keywords: *Star Formation: Massive – Maser – VLBI*

1 INTRODUCTION

Massive stars, or stars with mass more than $8M_{\odot}$, have important impacts in the history of the universe. Other than being a main luminosity sources in galaxies, they also impact their host galaxies evolution. Stellar wind from these starszz affects the turbulence in its environments. Their UV radiation ionizes gases and evaporates dust around them and drives flows and expansion motions of materials. Their death in the form of supernova explosion disturbs their neighbours but also enriches them with elements and compounds that could not be formed in other places and conditions. More processes influenced by this change in metallicity ranges from star formations to planet formation (Tan et al., 2014). In more general schemes, this will also affect the physical, chemical, and morphological structure of their host galaxies (Kennicutt et al., 1998, Kennicutt et al. 2005).

Even though this class of star is important for understanding the evolution of the universe, very much remains to be known about its formation and early evolution. Observation to these objects is hindered by their short evolution timescale, heavy interstellar absorption, clustering with other objects, and their very far distance (Tan et al., 2014). They are also rare according to stellar initial mass function (IMF) and spend about 15% of their entire lifetime in pre-main sequence (PMS) phase and then only a part of that in possible collapse and active accretion phase (Churchwell, 2002). These factors make observation very hard to be done, especially in their early phases.

The advance of interferometry techniques helps much to alleviate angular resolution problems caused by distance and close proximity to other objects. Tracers such as masers and emission lines are then used to circumvent extinction caused by dust and gases that shroud massive star formation region. Methanol masers are specifically used to trace massive star formation process (e.g., Fujisawa et al., 2014) and water masers are used to trace more general gas flow process such as outflow or expansion (e.g., Burns et al., 2017; Moscadelli et al., 2007). The problem of rarity as a consequence of massive stars short timescale and small portion in IMF distribution is overcome by the existence of large survey programs.

Maser object G354.61+0.47 is located at the Scorpius constellation with approximate ICRS coordinate of RA(J2000) 17^h 30^m 17.15^s and Dec.(J2000) -33° 13’ 54.8” (Csengeri et al., 2017a). It is located at the distance of 3.8 kpc (Green & McClure-Griffiths, 2011). Multiple masers have been observed in this object, such as OH maser (e.g. Caswell, 1998); and also CH_3OH for both Class I (e.g. Yang et al., 2017), and Class II (e.g. Fujisawa et al., 2014) using single-dish and interferometric observations. CH_3OH maser variability also was observed by Goedhart et al. (2004). Faúndez et al.

(2004) managed to detect infrared peak in the position of this object. ATLASGAL survey data is used to identifies a massive clump corresponding to this object that has high probability of being associated with a massive formation process (Csengeri et al, 2017b). Further analysis of ATLASGAL data by Urquhart et al. (2018) resulted in the parameters of this massive clump. Two massive cores are also identified and detected (Csengeri et al., 2017a) with one of them, core MM1, is associated with the maser distributions presented in this paper.

In this paper, we use KaVA observation to determine the proper motion and distribution of H_2O maser in G354.61+0.47. This data will then be compared to CH_3OH maser distribution taken with EAVN (Fujisawa et al., 2014). ALMA follow-up of ATLASGAL survey (Csengeri et al., 2017a) is also used to make dust continuum map and zeroth moment map of CO (*J=3*-2) emission line. In Section 2, we briefly explain the data source, instrumental configuration and data analysis process done. In Section 3, we present the proper motion and absolute motion measurements for H_2O maser. Comparison between H_2O and CH_3OH maser distribution is displayed. An additional comparison with ALMA data is also performed. Lastly, we discuss the possible interpretation of the available data and future prospects in Section 4.

2 OBSERVATIONS AND DATA ANALYSIS

2.1 H_2O Maser

Using the KaVA Array, the 6_{16}-5_{23} H_2O maser line (rest frequency 22,235.080 MHz) was observed at 7 epochs (17 January, 13 March, 8 May, 11 September, 13 October, 21 November 2019 and 7 January 2020). The continuum source NRAO530 was used as a bandpass calibrator.

The scan length for each object observed is around 5 minutes. Total integration time for G354.61+0.47 is around 1 hour. The data were correlated with Korea-Japan Joint VLBI Correlator (KJJVC).

The data were reduced using AIPS software. Digital sampling error were corrected. Calibration of clock and bandpass calibration were done by using NRAO530 as calibrator. After that, Doppler correction was performed for the maser line. Delay-rate calibration was performed by using spectral channel with the strongest maser channel. Maser spots are considered real if they have SNR (signal-to-noise ration) equal to or greater than 5 in two or more consecutive channels within FWHM (full-width at half-maximum) of the beam size around 3 milli-arcseconds (mas). Each collection of maser spots was then fitted using elliptical Gaussian and then collected as maser features with positions determined by the average of corresponding maser spots position. Data processing yielded a velocity coverage of 431 km s^{-1} and a channel spacing of 0.421 km s^{-1}. Absolute positions of maser features in this data have accuracy of roughly 50 mas.

Table 1. Summary of maser features in each epoch.

Epoch No.	Date	Feature Number	
		Northern	Southern
1	17 Jan. 2019	11	5
2	13 Mar. 2019	11	5
3	8 May 2019	8	2
4	11 Sept. 2019	1	-
5	13 Oct. 2019	1	-
6	21 Nov. 2019	5	-
7	7 Jan. 2020	3	-

2.2 CH_3OH Maser

Class II $5_1 - 6_0$ A^+ CH_3OH maser data (rest frequency 6,668.518 MHz) used in this research is taken during 2010 to 2011 EAVN observing session by Fujisawa et al. (2014) and appended by the data taken in 2012. The continuum sources 3C454.3 and NRAO530 are respectively used as fringe finder and bandpass calibrator. Absolute positions of maser features in this data have accuracy of roughly 200 mas.

Each scan lasted 15 minutes and was repeated three or four times with an interval of 1 or 2 hours, yielding the total integration time of around 1 hour. Data are then correlated in Mitaka FX correlator. Data processing yielded a velocity of coverage of 180 km s^{-1} and a channel spacing of 0.178 km s^{-1}. The typical size of the minor axis of the synthesized beam was 5 mas.

2.3 Dust Continuum and CO Line

Data used in this research is also taken from ALMA Archive with Project Code 2013.1.00960.S. This data is an end product of SPARKS project (Search for High-mass Protostars with ALMA up to

Table 2. Proper motion of seven features with detection in three or more epoch. Uncertainty is calculated from standard error of least-square fitting result. First column is feature code, the second is proper motion in right ascension and the last is proper motion in declination. All of proper motions are in mas yr^{-1}.

Code	$\mu_\alpha \cos\delta$	μ_δ
S1	-1.75 ± 0.96	1.79 ± 3.41
N1	-1.62 ± 0.97	7.39 ± 4.00
N2	-1.04 ± 0.94	-1.72 ± 1.96
N3	4.55 ± 3.36	0.72 ± 1.83
N6	-0.55 ± 0.94	-3.12 ± 1.64
N10	2.35 ± 4.13	-5.62 ± 8.33
N11	-1.94 ± 0.96	0.56 ± 1.71

kilo-parsec scales; e.g. Csengeri et al., 2018). Sources targeted in this project are mid-IR quiet massive clumps which are detected in APEX Telescope Large Survey of the Galaxy (ATLASGAL; Schuller et al., 2009, Csengeri et al., 2017a). Observations are conducted in Band 7 using 7 m and 12 m antennas. ALMA 12 m array observation whose result we use in this research has baselines ranged from 15 m (17 kλ) to 1574 m (1809 kλ). The four basebands used are centred in 347.331, 345.796, 337.061, and 333.900 GHz with spectral resolution of 0.977 MHz that corresponds to ~0.9 km s^{-1} in velocity resolution. Synthesized beam for the 12 m array is 0.70" × 0.45", with a geometric mean of 0.56" resolution (~2100 au;). For CO (J=3-2) data cube, resulting synthesized beam is 0.89" × 0.60", with a geometric mean of 0.73" resolution (~2800 au).

3 RESULTS

Analysis of H_2O maser data gives us maser features that are distributed roughly in two groups in intensity map. Those located near the brightest maser feature, whose channel used as fringe-fitting reference, is called Northern distribution and given code N. Other distribution located below the previous distribution in southwestern direction is called Southern distribution and given code S. The summary of detected maser features in each epoch is given in Table 1.

3.1 Proper Motion

Proper motion measurements were done for maser features detected in three or more epochs. Corresponding features in each epoch was matched by spatial and LSR velocity proximity criteria. Measurement was done using relative position data

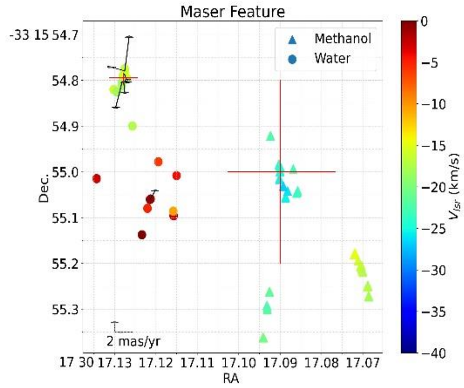

Figure 1. Map of H_2O (*circle*) and CH_3OH (*triangle*) maser distributions. Color code shows the LSR velocity values of the maser features. Arrows show proper motion values shown in Table 2. Red cross illustrates uncertainty in absolute position determinations.

before absolute position was determined. Reference position chosen was the brightest maser spot used in fringe-fitting calibration. Proper motion value was then obtained using ordinary least square fitting and its uncertainty is the standard error of the parameter. An average value of 0.43 ± 0.94 in right ascension and 4.13 ± 1.57 in declination were found from this initial data and then assumed as the systemic proper motion of all the maser features. Internal proper motion result was then found by subtracting this value from the initial result. Its values can be seen in Table 2.

3.2 Absolute Position

Fringe-rate mapping was utilized to determine the absolute coordinate of the H_2O maser features. Spectral channels used were corresponded to three peaks detected in autocorrelation spectrum of the first epoch data. Corresponding maser features offset from phase tracking centre were determined and

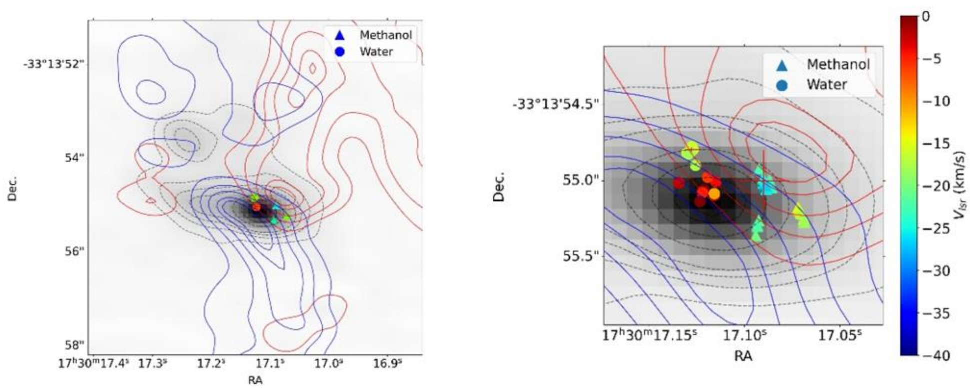

(a) (b)

Figure 2. (*a*) Map of ALMA Band 7 continuum taken by 12 m array (*grayscale, dashed contour*) overlaid by CO (J=3-2) integrated emission line in red-wing (*red*) and blue-wing (*blue*). Also in the map is H_2O (*circle*) and CH_3OH (*triangle*) maser features. Contour of 870 μm continuum and CO emission line respectively shows (5, 10, 15, 20, 40, 60, 80, 90) and (20, 40, 60, 80, 90) percent of the peak value. Close-up version showing maser distributions in great detail could be seen in (*b*). Details for maser features are the same with Figure 1.

used to get absolute position of maser features. Different results from each run of fringe-rate mapping were averaged to get the final result. Using maser features S1, N1 and N6 to determine the absolute positions, H_2O maser features distribution and its comparison with CH_3OH maser distribution can be seen in Figure 1.

3.3 Comparison with ALMA Data

Continuum imaging of ALMA 12 m array data was done using CASA. Zeroth moment map of CO (J=3-2) emission line was also produced. Using reference LSR velocity of -20.08 km s^{-1} from Wienen et al. (2015), we separated the line into blue- and red-shifted part and produced contour plots for both of them. This emission line describes bipolar outflow structures along the NW-SE direction in the object. A composite image containing the continuum map, the contour plots and maser distributions can be seen in Figure 2. It can be seen that the water masers are situated in red-wing contour and the methanol masers are located near the peak of the continuum map.

4 DISCUSSION AND CONCLUSION

The preceding results show a dynamical structure in G354.61+0.47. Owing the fact that 6.7 GHz CH_3OH masers trace massive star formations (Breen et al., 2013), comparison between dust continuum shown by ALMA 12 m array Band 7 continuum with methanol maser distribution and its roughly elliptical shape leads to the conclusion that this object harbour massive star formation. Its elliptical shape and LSR velocity distribution would lend credence to conclusion that this maser distribution traces circumstellar disk structure. Its shape and velocity show us the possibility that it could have some inclination relative to the line of sight.

The H_2O maser distribution result poses a very interesting problem. Its positions relative to CH_3OH distribution leads us to some interesting questions. Although its LSR velocity is in the range of those of a red-shifted outflow lobe, their positions and proper motions need some explanation. Scenario that agrees with available data is the possibility that it shows outflow launched from the edge of the disk (e.g., Hirota et al., 2017). The other conservative scenario is the possibility that the disk pole inclination gives us some geometric configuration that results in such distribution. A possible interpretation of the proper motion result in this scenario is that it shows decollimation process of the outflow/jet. The fact that there are two groups of H_2O masers with different LSR velocity also indicates possibility of episodic outflow (e.g., Burns et al., 2017). It is also possible that the H_2O maser distribution traces expansion or turbulent motion of the gases.

Similar analysis could be done to $C^{17}O$, SiO, SO_2 and CH_3OH spectral line emission data available in the ALMA data. A phase referencing observation to improve CH_3OH maser absolution position has also been proposed and awaiting approval. Further modelling and measurement will be done in future publication. In the future, Indonesia can participate in similar maser observations when Southeast Asian VLBI Network is operational.

7 REFERENCES

Breen, S. L., Ellingsen, S. P., Contreras, Y., Green, J. A., Caswell, J. L., Stevens, J. B., Dawson, J. R., et al., 2013, *Mon. Notices Royal Astron. Soc.*, 435, 524-530.

Burns, R. A., Handa, T., Imai, H., Nagayama, T., Omodaka, T., Hirota, T., Motogi, K., et al. 2017, *Mon. Notices Royal Astron. Soc.*, 467, 2367-2376.

Caswell, J. L. 1998, *Mon. Notices Royal Astron. Soc.*, 297, 215-235.

Churchwell, E. 2002, *Annu. Rev. Astron. Astrophys.,* 40, 27-62.

Csengeri, T., Bontemps, S., Wyrowski, F., Motte, F., Menten, K. M., Beuther, H., Bronfman, L., et al. 2017a, *A&A*, 600, L10, 9pp.

Csengeri T., Bontemps, S., Wyrowski, F., Belloche, A., Menten, K. M., Leurini, S., Beuther, H., et al. 2018. *A&A*, 617, A89, 17pp.

Faúndez, S., Bronfman, L., Garay, G., Chini, R., Nyman L.-Å. 2004, *A&A*, 426, 97-103.

Fujisawa, K., Sugiyama, K., Motogi, K., Hachisuka, K., Yonekura, Y., Sawada-Satoh, S., Matsumoto, N., et al. 2014, *PASJ*, 66, 31, 77pp.

Goedhart, S., Gaylard, M. J., van der Walt, D. J. 2004, *Mon. Notices Royal Astron. Soc.*, 355, 553-584.

Green, J. A., & McClure-Griffiths, N. M. 2011, *Mon. Notices Royal Astron. Soc.*, 417, 2500-2553.

Hirota, T., Machida, M. N., Matsushita, Y., Motogi, K., Matsumoto, N., Kim, M. K., Burns, R. A., et al., 2017, *Nat. As.*, 1, 0146, 16pp.

Kennicutt, R. C. 1998, *Annu. Rev. Astron. Astrophys.,* 36, 189-232.

Kennicutt, R. C. 2005, in *Massive Star Birth: A Crossroads of Astrophysics* (eds. R. Cesaroni, M. Felli, E. Churchwell, M. Walmsley), Cambridge University Press, Cambridge, 3-11.

Moscadelli, L., Goddi, C., Cesaroni, R., Beltrán, M. T., Furuya, R. S., et al. 2007, *A&A*, 472, 867-879.

Schuller, F., Menten, K. M., Contreras, Y., Wyrowski, F., Schilke, P., Bronfman, L., Henning, T., et al. 2009, *Astron. Astrophys*. 504, 415-427.

Tan, J. C., Beltrán M. T., Caselli, P., Fontani, F., Fuente, A., Krumholz, M. R., McKee, C. F., et al., 2014, in *Protostars and Planets VI* (eds. H. Beuther, R. Klessen, C. Dullemond, Th. Henning), University of Arizona Press, Tucson, 149-172.

Wienen, M., Wyrowski, F., Menten, K. M., Urquhart, J. S., Csengeri, T., Walmsley, C. M., Bontemps, S., et al. 2015. A&A, 579, A91, 35pp.

Yang, W., Xu, Y., Chen, X., Ellingsen, S. P., Lu, D., Ju, B., et al. 2017, *Astrophys. J., Suppl. Ser*. 231, 20, 12pp.